UC-38
LBL-20468
c.1

Lawrence Berkeley Laboratory

UNIVERSITY OF CALIFORNIA

RECEIVED
LAWRENCE
BERKELEY LABORATORY
NOV 20 1985
LIBRARY AND
DOCUMENTS SECTION

Accelerator & Fusion Research Division

Presented at the International Conference on Insertion Devices for Synchrotron Sources, Stanford, CA, October 27-30, 1985

PREDICTING THERMAL DISTORTION OF SYNCHROTRON RADIATION MIRRORS WITH FINITE ELEMENT ANALYSIS

R. DiGennaro, W.R. Edwards, and E. Hoyer

October 1985

For Reference

Not to be taken from this room

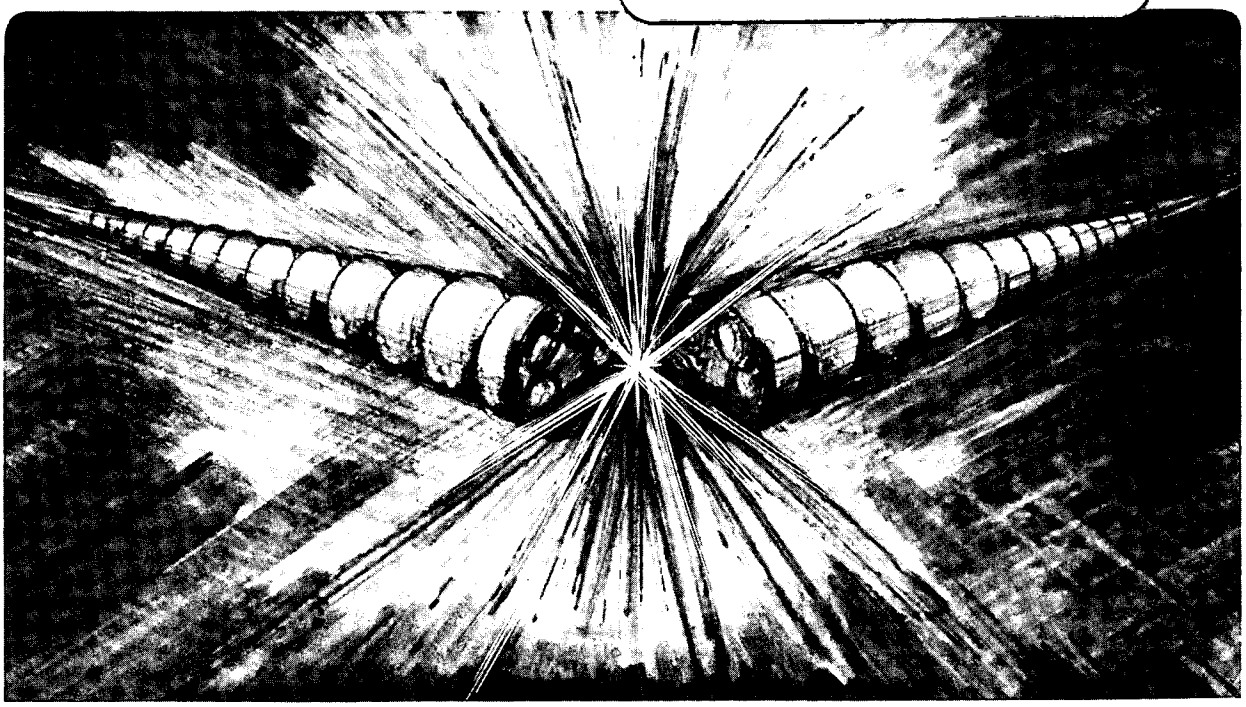

LBL-20468
c.1

Prepared for the U.S. Department of Energy under Contract DE-AC03-76SF00098

DISCLAIMER

This document was prepared as an account of work sponsored by the United States Government. While this document is believed to contain correct information, neither the United States Government nor any agency thereof, nor the Regents of the University of California, nor any of their employees, makes any warranty, express or implied, or assumes any legal responsibility for the accuracy, completeness, or usefulness of any information, apparatus, product, or process disclosed, or represents that its use would not infringe privately owned rights. Reference herein to any specific commercial product, process, or service by its trade name, trademark, manufacturer, or otherwise, does not necessarily constitute or imply its endorsement, recommendation, or favoring by the United States Government or any agency thereof, or the Regents of the University of California. The views and opinions of authors expressed herein do not necessarily state or reflect those of the United States Government or any agency thereof or the Regents of the University of California.

Predicting Thermal Distortion of Synchrotron Radiation Mirrors with Finite Element Analysis*

Richard DiGennaro, William R. Edwards, Egon Hoyer

Lawrence Berkeley Laboratory, University of California,
Berkeley, California 94720

Abstract

High power and high power densities due to absorbed radiation are significant design considerations which can limit performance of mirrors receiving highly collimated synchrotron radiation from insertion devices and bending magnet sources. Although the grazing incidence angles needed for x-ray optics spread the thermal load, localized, non-uniform heating can cause distortions which exceed allowable surface figure errors and limit focusing resolution.

This paper discusses the suitability of numerical approximations using finite element methods for heat transfer, deformation, and stress analysis of optical elements. The primary analysis objectives are (1) to estimate optical surface figure under maximum heat loads, (2) to correctly predict thermal stresses in order to select suitable materials and mechanical design configurations, and (3) to minimize fabrication costs by specifying appropriate tolerances for surface figure. Important factors which determine accuracy of results include finite element model mesh refinement, accuracy of boundary condition modeling, and reliability of material property data. Some methods to verify accuracy are suggested.

Design analysis for an x-ray mirror is presented. Some specific configurations for internal water-cooling are evaluated in order to determine design sensitivity with respect to structural geometry, material properties, fabrication tolerances, absorbed heat magnitude and distribution, and heat transfer approximations. Estimated accuracy of these results is discussed.

Synchrotron Radiation Mirror Design Issues

Optical surface distortion produced by non-uniform heat absorption can severely limit performance of x-ray mirrors for synchrotron radiation. High power and high power densities in photon beams from insertion devices and bending magnets can cause thermal distortions which exceed allowable surface figure errors and limit focusing resolution. Minimizing incidence angles and locating mirrors as far as possible from synchrotron sources reduces peak power density by distributing flux over greater surface area; however, economic and technological constraints limit allowable optical element size and beam line length.

Precise calculations to predict mirror thermal distortions are difficult due to the combination of (a) highly non-uniform heat absorption over the region of photon flux, (b) large thermal and structural volume needed for rigidity in polishing and mounting, and (c) high accuracy requirements for slope and surface figure errors. The range of surface deflections which determine acceptable optical performance is generally orders-of-magnitude smaller than for allowable deflections in traditional engineering systems. Calculation of thermal stresses and deflections must account for possible temperature variation of materia properties, and material strength must be judged in terms of an elastic limit which can be significantly lower than published "yield strength". Classical thermal stress-deflection analysis can be inadequate to predict performance and to insure against damage without costly over-design and specification of close fabrication tolerances.

R.T. Avery's summary of general thermal problems on high flux beam lines and specific design issues on LBL/Exxon/SSRL Beam Line VI suggests that classical analysis based on empirical formulas and engineering experience is satisfactory for many problems relating to transient and steady-state thermal stresses in beam line components.[1] As designers gain more experience with high flux and highly collimated synchrotron radiation from insertion devices, appropriate safety factors and design configurations will evolve toward better and less expensive thermal designs. However, there is limited experience with the problem of predicting and minimizing thermal distortion of optical surfaces for synchrotron radiation, and careful analysis is needed to help insure that optical performance meets specifications.

Finite element analysis

During the past 20 years, scientists and engineers have used finite element analysis (FEA) extensively for approximate solution of differential equations which describe a wide range of physical phenomena. FEA for thermal stress analysis was pioneered in the nuclear power industry, and more recently, it has been applied to diverse industrial problems such as heat transfer analysis for electronic devices and circuit boards in the semiconductor industry, thermal distortion and stress-deflection analysis for computer disc drives and high-power laser mirror systems.[2]

*This work was supported by the Office of Basic Energy Research, U.S. Department of Energy, under Contract #DE-AC03-76SF00098.

The general benefit of FEA is to enable designers to solve analytically design problems for situations in which classical analysis is inadequate or impossible. Such problems would otherwise be resolved by experimental means and conservative safety factors - making it difficult to produce cost-effective designs. For predicting optical surface distortion and thermal stresses in a synchrotron radiation mirror, FEA enables designers to evaluate alternate design configurations and materials at a small fraction of the cost of building and testing prototypes.

Using FEA, an analyst represents a mechanical system with a geometric model composed of a finite number of pieces ("elements"), each of which approximates a discrete volume of a continuum. Governing equations for mechanical and physical behavior are assumed to apply uniformly within an element. Boundary conditions and element interactions occur at a discrete number of points ("nodes") which define the finite element (FE) mesh model.[3]

FE results are described in terms of degrees of freedom at nodes and representative mechanical behavior of elements. In thermal analysis, temperature is the only degree of freedom at nodes, and heat flux describes mechanical behavior of elements. In stress analysis, deflections at nodes occur with up to six degrees of freedom, and stresses and strains describe behavior. Number, size, shape, and distribution of elements ("mesh refinement") in the geometric model influence accuracy of approximations as well as overall computational costs. Reliability of results, judged by how well a model predicts mechanical behavior, depends largely on an analyst's ability to accurately describe material properties, boundary conditions, and geometric shape of the physical structure.

FE calculations require an independent check of their accuracy and reliability. An analyst may choose to rely on personal experience and intuition to judge computational results, but most experienced FE analysts recommend comparison, whenever possible, with approximate solutions such as calculations based on empirical formulas taken from engineering handbooks. A series of FE models with increasing complexity and mesh refinement can confirm accuracy of FE numerical approximations and reliability in comparison with formulas and observed prototype behavior. Evaluating results based on the full range of uncertainty for material properties, fabrication tolerances, and boundary conditions can be effective in judging reliability and sensitivity to specific loads and design features.

Finite element models for a synchrotron radiation mirror

Design efforts are in progress for a new branch on LBL/Exxon/SSRL Beam Line VI for photon energies in the vacuum ultra-violet (VUV) range - approximately 50 to 1000 eV. The first mirror, M-Zero, is to be located 8.8 meters from the 54-pole wiggler, with a horizontal deflection angle of 5.6 degrees. Angular collection aperture of M-Zero is 1.1 mRad, and for SPEAR in the maximum power mode of 3.0 GeV electron energy and 200 mAmp current, with peak magnetic field of 1.75 Tesla in the wiggler, M-Zero receives up to 2.4 kW of power. The mirror optical surface is approximately 200 mm (horizontal) by 20 mm (vertical) with a peak absorbed power density of 5.2 W/sq.mm.[4]

M-Zero has a flat surface figure, and maximum heat loads require direct cooling in order to maintain acceptable figure error. The configuration selected for M-Zero is a brazed, box-like assembly, with machined water channels beneath the optical surface, shown in Figure 1.

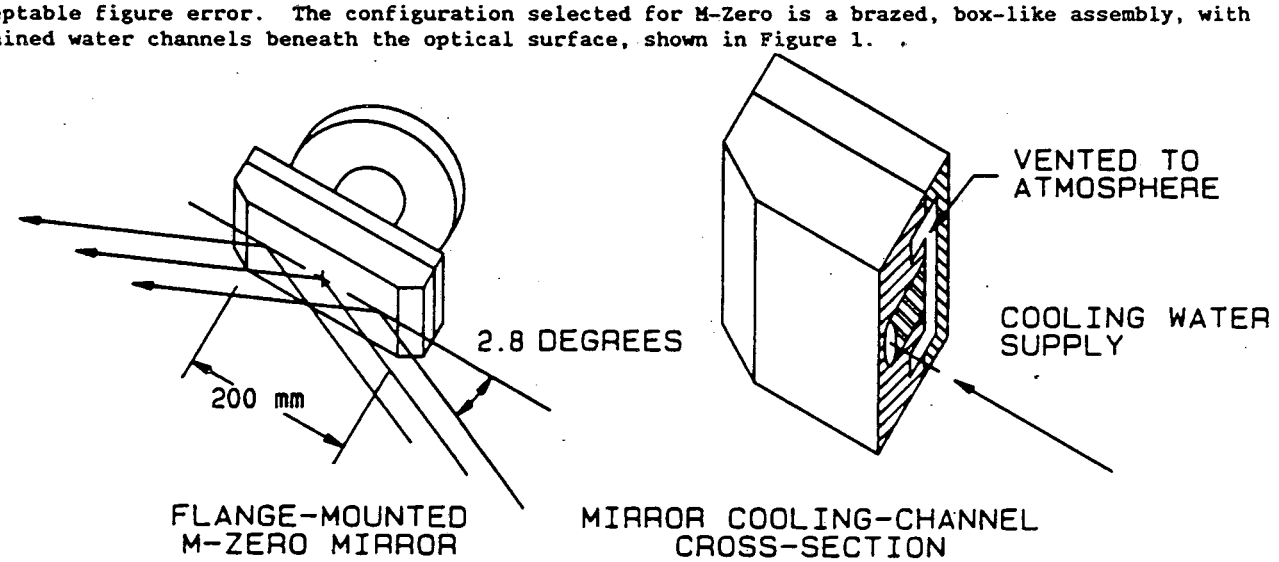

Figure 1. M-Zero Design Configuration. The mirror is a brazed, box-like assembly with a machined water channel beneath the optical surface. A separate mask (not shown) prevents beam impingement on the front end of the mirror.

A primary design objective for M-Zero is to avoid complexities which not only increase cost but also increase risk of problems in fabrication and operation. Prototype design configurations have been based on a single cooling channel parallel to the beam axis. The cooling channel receives water which is routed

from a single flange on the back of the mirror, with tubing connections for supply and return.

(1) Temperature distribution and in-plane distortion using plane strain model

Finite element analysis was performed for 3 general categories of approximations: A 2-dimensional model with relatively fine mesh density represents a cross-section of M-Zero, perpendicular to the optical surface, shown in Figure 2. For a unit-thickness of material, heat flux and thermal expansion are constrained in the plane of the model, which describes a 3-dimensional stress state in which there is no significant increase in mirror length due to heating. With a relatively fine mesh model, numerical approximations for computing temperature distribution and in-plane surface distortion are expected to be reasonably accurate; however, computed stress magnitudes are somewhat higher for this model. Actual longitudinal expansion, size, and mirror-mounting constraints will affect true stress. Reliability of computed slope errors along the transverse (vertical) optical surface is limited primarily by accuracy of boundary conditions (e.g., absorbed heat flux magnitude and distribution, heat loss, and thermal and structural behavior of brazed connections and gaps) and reliability of material property data (e.g., coefficient of thermal expansion, elastic modulus, thermal conductivity, and effects of temperature variation on material properties).

(2) Stress Distribution and Strain Using 3-Dimensional Model

A 3-dimensional model representing 1/4 of M-Zero is shown in Figure 3. Although a coarse mesh model is necessary to keep computational costs reasonable, it describes a true stress state because 3-dimensional heat flux, heat conductance, and thermal distortion are calculated. Coarse mesh approximations limit absolute accuracy, especially for computation of slope error for optical precision; however, computed stress magnitudes provide a valuable estimate for the safety factor inherent in plane strain approximations.

(3) Minimum stress estimates using plane stress model

A 2-dimensional model which has identical geometry and mesh refinement as the plane strain approximation shown in Figure 2 describes a cross-section of M-Zero allowed to expand freely in the longitudinal (normal) direction. This approximation assumes that there are no constraints acting normal to the plane of the model. Since actual constraints are expected to significantly limit longitudinal thermal expansion, the main objective for using a plane stress model is to describe an absolute lower limit for stress estimates, for comparison only.

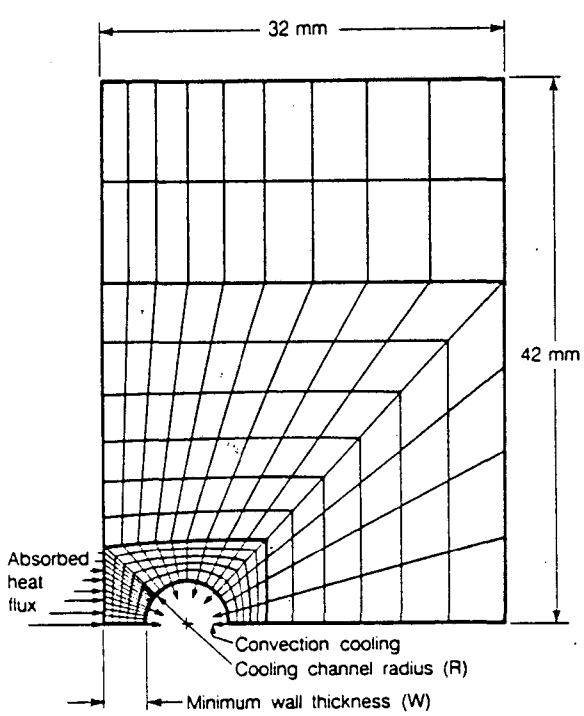

Figure 2. 2-Dimensional Mesh Model. The model describes a cross-sectional plane of the mirror, perpendicular to the optical surface. With the mirror centered vertically in the synchrotron beam, finite element calculations utilize the symmetry plane and model 1/2 of the mirror cross-section. For thermal analysis, heat flux is constrained to the plane of the model, and for plane strain analysis, normal stresses act to constrain all distortions to the plane of the model (i.e., no longitudinal expansion of the mirror).

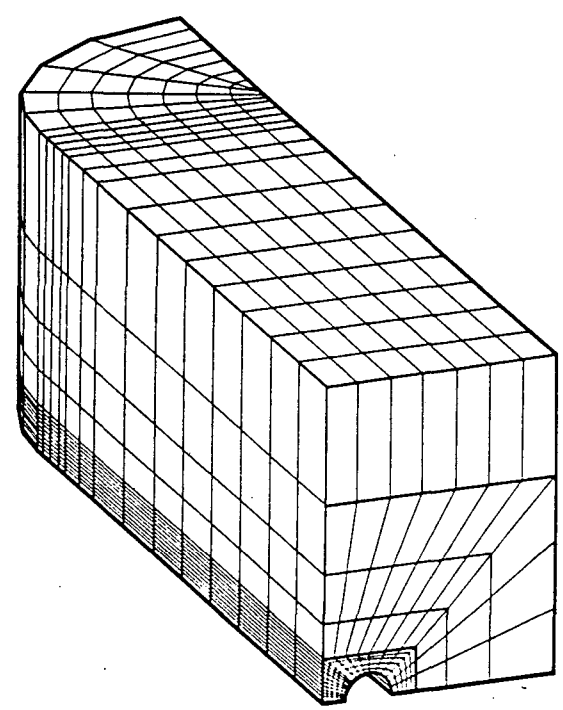

Figure 3. 3-Dimensional Mesh Model. Using symmetry, 1/4 of the mirror is modeled for calculation of 3-dimensional heat flux, distortions, and stresses, giving a reasonably accurate model of the true stress state for thermal loading of the mirror.

Finite element analysis design sensitivity calculations

Using FEA, design sensitivity was evaluated for the following parameters in order to estimate M-Zero stresses and optical performance and to select a design configuration and material.

(1) Material properties

Material properties which significantly affect thermal stress-deflection behavior are thermal expansion coefficient α, elastic modulus (E), and Poisson's ratio ν. For a given geometry and temperature distribution, thermal stresses are proportional to $(E\alpha)/(1-\nu)$. In M-Zero, high compressive stresses occur at or near the optical working area as a result of highly concentrated heat flux and large structural mass. The heated zone is constrained from expansion by the relatively cold structural volume. A material with low elastic modulus, low thermal expansion coefficient, and high Poisson's ratio will tend to have low thermal stresses.

High thermal conductivity (k) is especially important for M-Zero due to high peak power densities in the synchrotron beam and highly non-uniform power distribution. Thermal conductivity determines how effectively absorbed heat is removed from the heated zone: high conductivity results in small temperature gradients in the local volume of material which, in effect, reduces deformation of the optical working area. Non-uniform thermal expansion due to variations in temperature across the local structural volume is primarily responsible for distortion of the optical surface.

Using a plane strain FE model with a 3 mm minimum wall thickness, 3 mm cooling passage radius, and convective heat transfer film coefficient of 0.023 W/sq.mm-°C (for 20 ft/sec water flow rate), temperature distribution, surface distortion, and thermal stresses were computed for several potential mirror materials and a range of power intensities (Gaussian distribution with FWHM = 1.0 mm). Results are summarized in Figures 4A, 4B, and 4C, based on the following material property data:

Potential Mirror Materials
Property Data for Thermal Stress Analysis

Material	Thermal conductivity (w/mm-°C) k	Thermal Expansion Coefficient (per °C) α	Deformation Figure of merit $\frac{\alpha}{k}$	Elastic Modulus (psi) E	Poisson's ratio ν	Thermal Stress Figure of merit $E\alpha/k(1-\nu)$
		$\times 10^{-6}$	$\times 10^{-4}$	$\times 10^{6}$		
OFHC Copper	0.399	17.7	44.4	17.0	.33	1130
Cu Alloy C15715	0.365	16.6	45.5	16.0	.33	1090
Molybdenum	0.145	5.35	36.9	45.5	.32	2470
Beryllium	0.151	11.5	76.2	42.0	.03	3300
Al Alloy A356-T6	0.159	21.4	1.35	10.0	.33	2010
Silicon Carbide	0.105	3.50	33.3	35.0	.30	2290

Figures 4A, 4B, and 4C show that temperatures, slopes, and stresses are directly proportional to peak power density, based on a Gaussian distribution for absorbed power. Further, these calculations show that maximum surface temperature varies inversely with thermal conductivity k; maximum slope error (derived from thermal strain) varies with the deformation figure-of-merit factor α/k; and maximum thermal stress varies with the stress figure-of-merit factor $(E\alpha)/k(1-\nu)$.

Material properties are assumed to be constant in the temperature ranges considered. For materials with lower thermal conductivity, surface temperatures may be high enough to cause some temperature variation in material properties.

All stress calculations are presented as Von Mises equivalent stress, which is the most widely accepted failure criteria for yielding of ductile metals, for comparison with yield strength data from standard tensile tests.[5,6] These stress values are not strictly appropriate for predicting failure of brittle materials such as silicon carbide, but are used for comparison of the potential mirror materials.

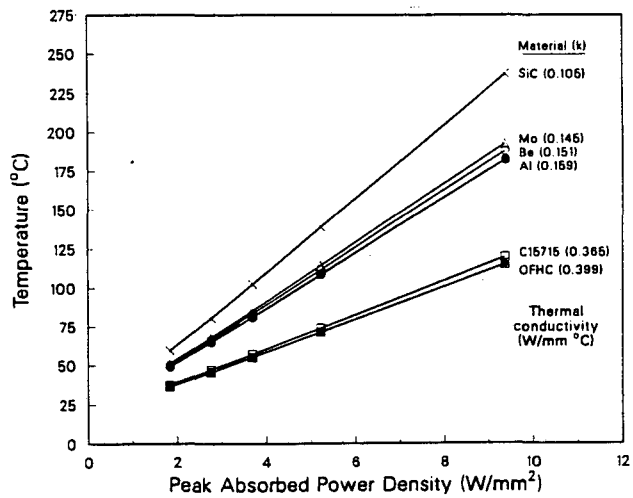

Figure 4A. Maximum Surface Temperatures. For a range of power levels, assuming a Gaussian absorbed heat distribution, FE calculations show that maximum surface temperatures vary inversely with thermal conductivity. Calculations are based on a nominal configuration (W = 3 mm, R = 3 mm) and convective heat transfer film coefficient (0.023 W/sq.mm-°C at 20 ft/sec water flow rate).

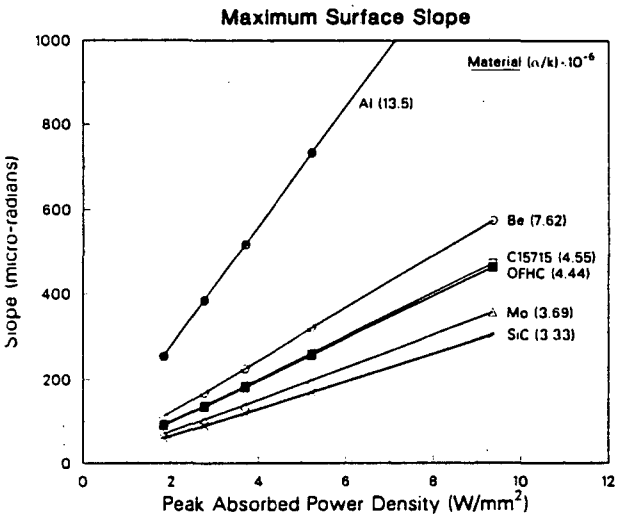

Figure 4B. Maximum Surface Slope. Figure error due to thermal distortion varies nearly linearly with a deformation figure-of-merit, k/α.

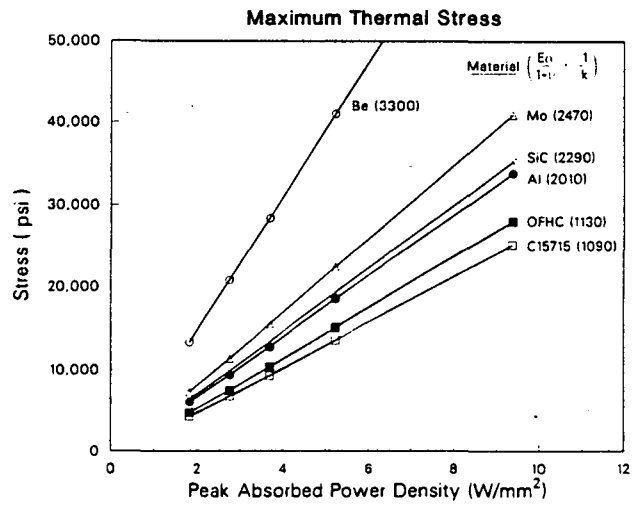

Figure 4C. Maximum Thermal Stresses. Von Mises Equivalent stresses, which are derived from principal stresses, vary nearly linearly with a thermal stress figure-of-merit, (Eα)/k(1 -ν).

For M-Zero, according to these calculations, Molybdenum, Silicon Carbide, OFHC Copper and Alumina Dispersion-strengthened Copper Alloy (UNS C15715)[7] give satisfactory performance for maximum slope error due to thermal distortion. Molybdenum and Silicon Carbide give the smallest slope error, but mirror fabrication with these materials for the configuration required appears to be quite costly.

At the nominal grazing incidence angle of 2.8°, peak power density on M-Zero exceeds 5 W/sq.mm which causes thermal stresses greater than the OFHC yield strength. Published yield strength for annealed alloy C15715 is 47,000 psi, which gives a safety factor of about 4 for this alloy, according to these plane strain calculations. (Additional tensile tests are planned in order to confirm that the true elastic limit for optical surface distortion is high enough to prevent any permanent deformation). Machinability of C15715, polishability[8], dimensional stability[9], and UHV outgassing characteristics after vacuum furnace brazing[10] are similar to OFHC. The C15715 alloy allows fabrication using conventional vacuum furnace brazing techniques. Hence, C15715 appears as a promising material for synchrotron mirrors which require direct cooling in high flux beam lines such as Beam Line VI.

(2) Geometry: minimum wall thickness and cooling channel radius

M-Zero has a single, machined channel for water-cooling near the heated surface. For this basic design configuration, minimum wall thickness and channel shape are the primary geometric parameters which determine maximum stress and surface slope.

Decreasing wall thickness reduces maximum surface temperatures and reduces wall temperature drop by decreasing heat conduction distances. However, decreasing wall thickness also reduces effective surface area for convection cooling and can increase temperature gradients near the optical surface.

For a constant cooling channel radius (R) of 3.5 mm and a convective heat transfer film coefficient of 0.023 W/sq.mm-°C, maximum surface slopes and thermal stresses for minimum wall thicknesses (W) between 0.5 and 10 mm are shown in Figures 5A and 5B for copper alloy C15715. These FE results show that surface distortion increases as W decreases below about 3 mm, with a corresponding increase in maximum thermal stress. In this range of W, effective area for convective cooling is highly localized, causing large temperature gradients which produce nonuniform thermal expansion. Also, free expansion is highly constrained by structural forces from the surrounding colder material, which increases maximum stresses.

Increasing W above 3 mm does not significantly reduce surface slope; however, maximum stress increases slightly. With increasing wall thickness, temperature distribution near the optical surface does not change significantly, but overall wall temperature drop does increase, causing higher thermal stresses.

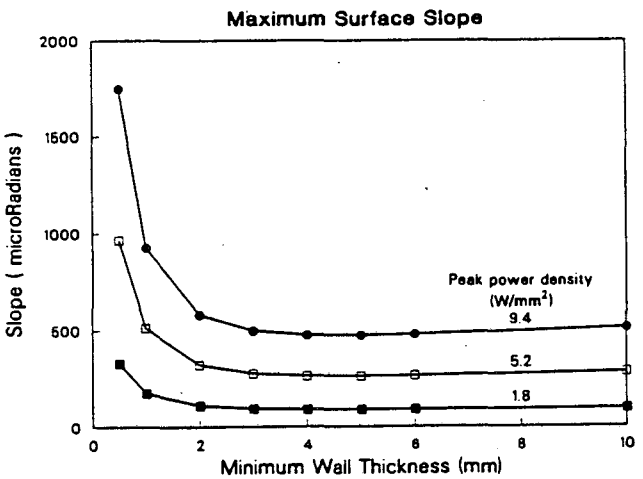

Figure 5A. Maximum Surface Slope. Thermal distortion at 3 different power levels is relatively insensitive to wall thickness with W greater than about 3 mm. Slope error increases significantly as wall thickness decreases below 3 mm. These FE calculations are for copper alloy C15715.

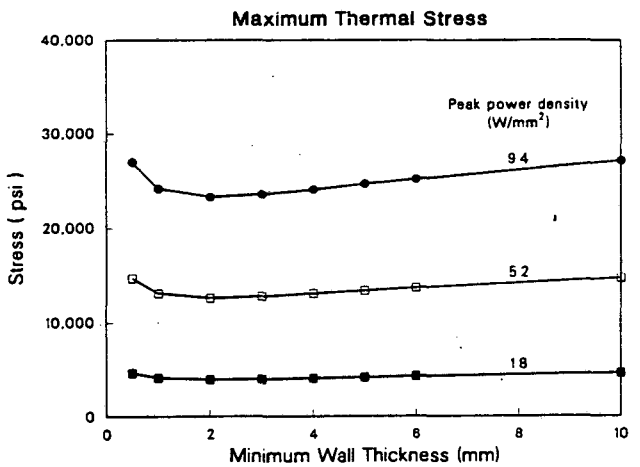

Figure 5B. Maximum Thermal Stress. Stresses do not vary significantly with changes in wall thickness; however, an apparent minimum stress level occurs at W = 2 mm for a cooling channel radius R = 3.5 mm.

Figures 6A and 6B show slope errors and stresses for cooling channel radius (R) between 2 and 6 mm and convective heat transfer film coefficient of 0.023 W/sq.mm-°C, with constant W of 3 mm. It is observed that larger R, which increases the effective area for convective cooling, reduces maximum thermal stresses. Larger R reduces the local structural volume of material which constrains thermal expansion, and surface distortion increases. Design selection of an appropriate cooling channel radius must compromise maximum stress and slope error - based on allowable stress for the material, fabrication costs, cooling water pressure, flow rate limits, etc.

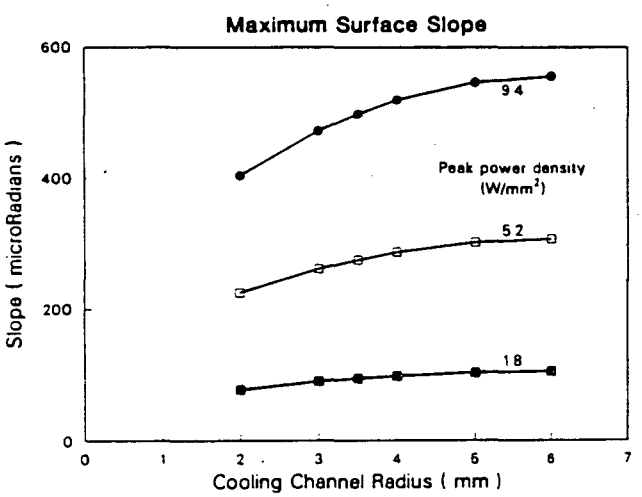

Figure 6A. Maximum Surface Slope. For a minimum wall thickness of 3 mm, thermal distortion increases as the cooling channel increases from 2 to 5 mm, for alloy C15715 at 3 power levels; maximum slope error increases by nearly 40%.

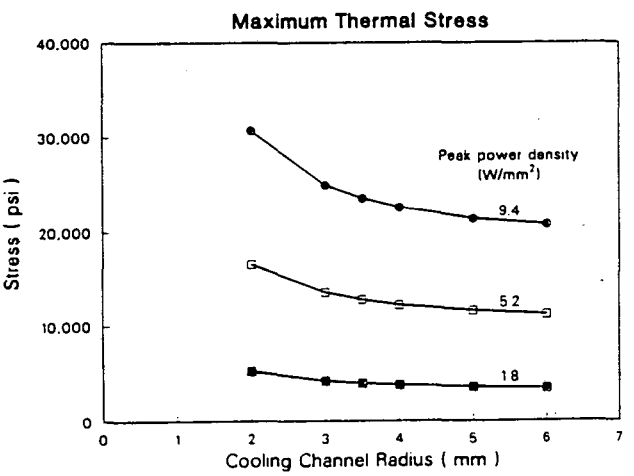

Figure 6B. Maximum Thermal Stress. Von Mises Equivalent Stresses decrease by about 30% as the cooling channel radius increases from 2 to 5mm.

In addition to the geometric parameters for minimum wall thickness and cooling channel shape, overall mirror dimensions are also significant for structural rigidity; however, small variations in these dimensions are not expected to affect thermal stress-deformation behavior and optical performance. The 2-dimensional FE calculations also do not consider end effects where there is an abrupt change in heat flux. 3-dimensional FE models are required to determine an appropriate geometric configuration for mirror ends. Mounting constraints are neglected since the actual mounting is structurally isolated from the bulk volume in order to prevent clamping forces from causing any surface figure distortion. Forces due to internal water pressure (125 psi) are small, but cause a slight decrease in maximum stress and surface distortion due to the tensile "hoop stress" which compensates for some of the compressive thermal stress.

(3) Thermal boundary conditions: heat flux and convection cooling uncertainties

Reliability of FE predictions for optical performance depends on how well an analyst models actual boundary conditions. Uncertainties in the following thermal boundary conditions for M-Zero largely determine the probable error in FE results:

(a) Theoretical photon flux and power distribution in synchrotron radiation are readily computed for point source-size approximations.[11,12] Additional corrections may be made to account for finite source size.[13]

(b) Theoretical reflectance characteristics for optical coating type and beam incidence angle are used to estimate total power absorbtion and absorbed power densities.[14]

(c) Empirical formulas such as the Sieder-Tate equation for convective heat transfer through a turbulent boundary layer estimate direct cooling effectiveness.[15]

(d) Additional heat loss by radiation from exposed surfaces, loss of absorbed synchrotron radiation due to photoelectric emission, and by conduction through mounting supports may be included in calculations.

(e) Mis-alignment effects such as a vertically mis-steered beam or mis-aligned mirror may significantly change optical performance and potentially damage the mirror.

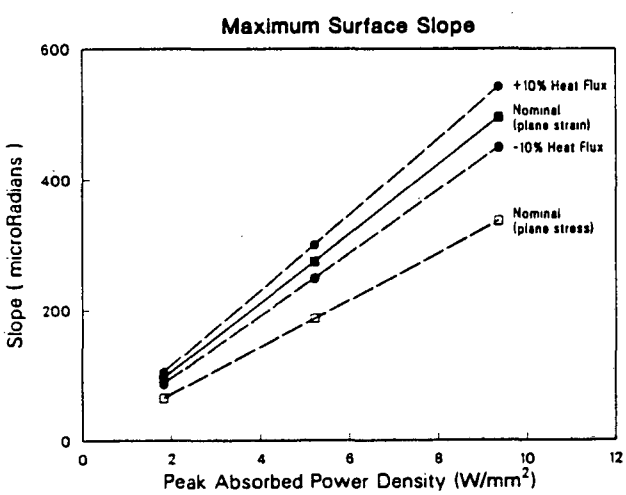

Figure 7A. Maximum Surface Slope. M-Zero slope error based on plane strain approximations varies by ±9% as the thermal boundary conditions (heat flux and convective film coefficient) vary by ±10% for copper alloy C15715, W = 3mm, R = 3.5mm.

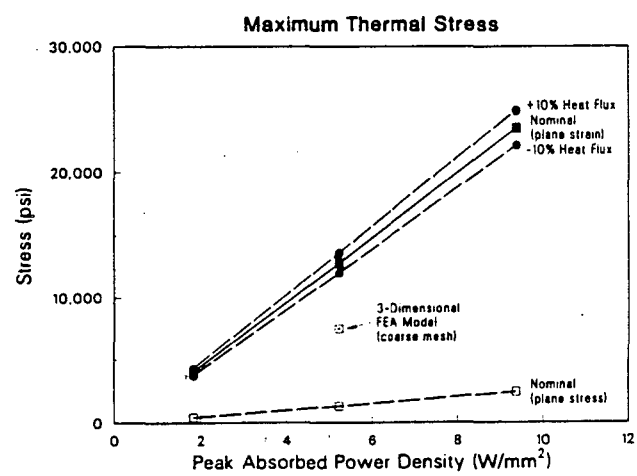

Figure 7B. Maximum Thermal Stress. Computed stress is highest using the plane strain approximation, and ±10% variation in the thermal boundary conditions coefficient) (heat flux and convective film cause a ±7% variation in stress. For M-Zero at maximum power (5.2 W/sq.mm), the 3-dimensional calculation provides the best estimate for actual stresses.

M-Zero mirror design

Thermal stresses and surface slopes shown in Figures 7A and 7B represent FE calculations for a nominal M-Zero geometry (W = 3 mm and R = 3.5 mm) and a range of FE model approximations, including plane stress, plane strain, 3-dimensional FE approximations, and sensitivity of the plane strain model to variations of ±10% for the thermal boundary conditions (heat flux and convection film coefficient). Heat loss by radiation and conduction is neglected, and cooling by the return water channel is also ignored. Water is assumed to be at a uniform temperature of 18°C.

Computed stresses are highest using a plane strain model, predicting maximum stress for M-Zero to be nominally 12,800 psi. Actual stresses are expected to be close to the values predicted by the 3-dimensional calculation: a peak power density of 5.2 W/sq.mm on M-Zero produces a maximum thermal

stress of approximately 7500 psi. The plane strain sensitivity results indicate that the stress results are reliable within ±7% for the ±10% variation in the heat flux and convection coefficient. (The plane stress FE model is not a reliable representation of the true stress state, since it ignores any longitudinal constraining forces, and it is included for comparison only.)

Transverse (vertical) slope calculations for the plane strain FE model are expected to be more reliable than the 3-dimensional calculations due to the finer mesh density used for the 2-dimensional calculations. Maximum surface slope error for the nominal condition is 276 microradians, with variation of ±9% for the ±10% variation in heat flux and convection film coefficient.

Heat flux for these FE calculations was determined using a point-source approximation, which describes the highest possible power density. The mirror is positioned at the center of the synchrotron beam, receiving the maximum power density and total power. Effects of mis-alignment are not considered.

Conclusions

1. Using copper alloy C15715 for the M-Zero mirror, maximum thermal stresses at the highest anticipated power levels will be less than 10,000 psi, according to finite element calculations. Based on published yield strength, the safety factor is about 6. Maximum surface slope error due to thermal distortion will be less than 300 microradians.

2. Finite element analysis was used to predict thermal stresses and surface distortion for a range of geometric configurations for a water-cooling channel in M-Zero. Minimum wall thickness of 3 mm and cooling channel radius of 3.5 mm were found to give a reasonable compromise between maximum stress and slope error for alloy C15715.

3. Design sensitivity of M-Zero to a range of thermal boundary conditions was evaluated using a plane-strain FE model: for ±10% variation in heat flux magnitude and convection film coefficient, maximum stress varies by ±7%, and maximum slope varies by ±9%.

4. These results are based on FE calculations only, and although manual calculations have verified that the results are reasonable, measurements of actual prototype behavior are not yet available. Evaluation of mirror performance in a synchrotron beam line is needed to confirm the validity of the predicted stresses and surface distortion.

Acknowledgements

We wish to acknowledge the suggestions and encouragement from Malcolm Howells at LBL for these design studies; and we want to thank Bill Lowry of CVI Laser Corp., Albuquerque, N.M., who provided helpful suggestions on mirror design and polishing. Finite element calculations were done using the ANSYS computer program by Swanson Analysis Systems, Inc.

References

1. R. T. Avery, Nucl. Instr. and Meth. 222 (1984) 146-158.
2. D. E. Dietrich, Ansys Conference Proceedings, April 23-25, 1985, Swanson Analysis Systems, Inc., Houston, Pennsylvania.
3. O. C. Zienkiewicz, and K. Morgan, Finite Elements and Approximations, (John Wiley & Sons, Inc., 1983).
4. E. Hoyer, Beam Power Apportionment, calculations, LBL note LBID-1063, September 1985.
5. J. E. Shigley, Mechanical Engineering Design, 3rd Ed., (McGraw-Hill, Inc., 1977).
6. E. P. Popov, Introduction to Mechanics of Solids, (Prentice-Hall, Inc., 1968).
7. UNS Alloy C15715 is a proprietary alloy ("GlidCop AL-15") by SCM Metal Products, Chemicals Division of SCM Corp., 1468 W. 9th Street, Cleveland, Ohio, 44113. It is a copper alloy which contains 0.15% (by weight) aluminum oxide particles, and strengthening is achieved by dispersion of the particles which act as barriers to dislocation movement, according to the manufacturer. A low-oxygen version can be exposed to hydrogen at high temperatures without embrittlement.
8. R. DiGennaro, Polishability and Substrate Evaluation, polishing test results, LBL note LBID-1061, April, 1985.
9. R. DiGennaro, Dimensional Stability of Alumina Dispersion-strengthened Copper Alloy, test results, LBL note LBID-1062, July, 1985.
10. K. Kennedy, LBL, desorption test results, not yet published.
11. G. Brown, K. Halbach, J. Harris, and H. Winick, Nucl. Instr. and Meth. 208 (1983) 65.
12. E. M. Lent and W. C. Dickinson, Spatial Distribution of Radiation from the Beam Line VIII-W 15-Period Wiggler, UCRL-53635, Lawrence Livermore National Laboratory, Univ. of Calif., Livermore, Calif. (May 1985).
13. E. Hoyer, ibid.
14. B. L. Henke, et al, Atomic Data and Nuclear Data Tables, Low Energy X-Ray Interaction Coefficients, Vol. 27, No. 1, (Academic Press, Jan. 1982).
15. E. N. Sieder and G. E. Tate, Ind. Eng. Chem. 28 (1936) 1429.

This report was done with support from the Department of Energy. Any conclusions or opinions expressed in this report represent solely those of the author(s) and not necessarily those of The Regents of the University of California, the Lawrence Berkeley Laboratory or the Department of Energy.

Reference to a company or product name does not imply approval or recommendation of the product by the University of California or the U.S. Department of Energy to the exclusion of others that may be suitable.

LAWRENCE BERKELEY LABORATORY
TECHNICAL INFORMATION DEPARTMENT
UNIVERSITY OF CALIFORNIA
BERKELEY, CALIFORNIA 94720